Evidence for a Proton Transfer Network and a Required Persulfide-Bond-Forming Cysteine Residue in Ni-Containing Carbon Monoxide Dehydrogenases†

Eun Jin Kim,‡ Jian Feng,‡ Matthew R. Bramlett,§ and Paul A. Lindahl*,‡,§

Departments of Chemistry and of Biochemistry and Biophysics, Texas A&M University, Post Office Box 30012, College Station, Texas 77842-3012

Received November 18, 2003; Revised Manuscript Received March 17, 2004

ABSTRACT: Carbon monoxide dehydrogenase from *Moorella thermoacetica* catalyzes the reversible oxidation of CO to CO_2 at a nickel−iron−sulfur active site called the C-cluster. Mutants of a proposed proton transfer pathway and of a cysteine residue recently found to form a persulfide bond with the C-cluster were characterized. Four semiconserved histidine residues were individually mutated to alanine. His116 and His122 were essential to catalysis, while His113 and His119 attenuated catalysis but were not essential. Significant activity was "rescued" by a double mutant where His116 was replaced by Ala and His was also introduced at position 115. The activity was also rescued in double mutants where His122 was replaced by Ala and His was simultaneously introduced at either position 121 or position 123. Activity was also rescued by replacing His with Cys at position 116. Mutation of conserved Lys587 near the C-cluster attenuated activity but did not eliminate it. Activity was virtually abolished in a double mutant where Lys587 and His113 were both changed to Ala. Mutations of conserved Asn284 also attenuated activity. These effects suggest the presence of a network of amino acid residues responsible for proton transfer rather than a single linear pathway. The Ser mutant of the persulfide-forming Cys316 was essentially inactive and displayed no electron paramagnetic resonance signals originating from the C-cluster. Electronic absorption and metal analysis suggest that the C-cluster is absent in this mutant. The persulfide bond appears to be essential for either the assembly or the stability of the C-cluster, and possibly for eliciting the redox chemistry of the C-cluster required for catalytic activity.

Ni-containing CODHs[1] are found in methanogenic archaea, acetogenic bacteria, and CO-utilizing bacteria, where they play critical roles in C_1 metabolism (*1*). This family of enzymes catalyzes the reaction

$$CO + H_2O \rightleftarrows CO_2 + 2e^- + 2H^+ \qquad (1)$$

The enzymes from *Rhodospirillum rubrum* ($CODH_{Rr}$) and *Carboxydothermus hydrogenoformans* ($CODH_{Ch}$) are β_2 homodimeric, while that from *Moorella thermoacetica* ($CODH_{Mt}$) is an $\alpha_2\beta_2$ tetramer in which the β subunits are homologues to those of $CODH_{Rr}$ and $CODH_{Ch}$. $CODH_{Mt}$ is bifunctional and also catalyzes the synthesis of acetyl-CoA. This paper focuses on reaction 1, and acetyl-CoA synthase aspects will not be discussed.

Reaction 1 occurs at the C-cluster, a novel structure divisible into a $[Fe_3S_4]$ subsite and a [Ni Fe] subsite (Figure 1). Two of the three facial sulfides of the $[Fe_3S_4]$ subsite coordinate the Ni while the third coordinates the unique Fe of the [Ni Fe] subsite. Four structures have been reported (*2*−*5*), including one each of $CODH_{Ch}$ and $CODH_{Rr}$ and two of $CODH_{Mt}$. Structures are grossly equivalent, although there are minor differences that may be functionally significant. The C-cluster of $CODH_{Mt}$ as reported by Darnault et al. is structurally heterogeneous (*5*). One aspect of that heterogeneity was that a portion of the molecules contains a persulfide bond between a sulfide ion of the $[Fe_3S_4]$ subsite and the sulfur of Cys316 (Figure 1, structure on right). The remaining C-cluster molecules lack this persulfide and have Cys316 or its equivalent uncoordinated, as represented by the structure on the left in Figure 1. Whether the persulfide bond plays a role in catalysis or is simply an artifact of protein purification or crystallization is not known, but Cys316 is

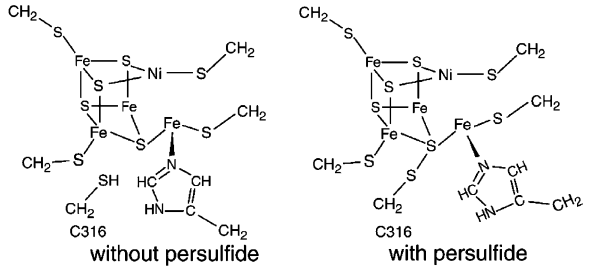

FIGURE 1: Idealized structures of the C-cluster from *M. thermoacetica* (*5*), with (right side) and without (left side) the persulfide bond.

† This work was supported by the National Institutes of Health (Grant GM46441) and the Department of Energy (Grant DE-F603-01ER15177). The National Science Foundation provided funds for the EPR spectrometer (CHE-0092010).

* To whom correspondence should be addressed. Tel: 979-845-0956. Fax: 979-845-4719. E-mail: Lindahl@mail.chem.tamu.edu.

‡ Department of Chemistry.

§ Department of Biochemistry and Biophysics.

[1] Abbreviations: CODH, carbon monoxide dehydrogenase; $CODH_{Rr}$, CODH from *R. rubrum*; $CODH_{Ch}$, CODH from *C. hydrogenoformans*; $CODH_{Mt}$, CODH from *M. thermoacetica*; EPR, electron paramagnetic resonance; WT, wild-type.

10.1021/bi036062u CCC: $27.50
Published on Web 04/24/2004

Table 1: Sequence of Amino Acids (Deduced from Nucleotide Sequencing) for Various CODHs, Adapted from Ref *6*; Residue Numbering for $CODH_{Mt}$ Is Assumed

Organism	Residue Number			
	112 – 126	282-285	314-318	586-588
M. thermoautotrophicum	AHAGHARHLVDHLIE	GHNV	GICCA	QKA
M. jannaschii I	CHAGHSRHLVHHLIE	GHHA	GICCT	QKA
A. fulgidus I	AHTGHARHML…HDIE	GHNV	GLCCT	QKA
M. frisia I	CHAAHGRHLLDHLIE	GHNV	GLCCT	QKA
M. frisia II	CHAAHGRHLLDHLIE	GHNV	GICCT	QKA
M. thermophila	CHAAHGRHLLDHLIE	GHNV	GVCCT	QKA
M. soehngenii	AHTAHGRHLY…HWCL	GHNL	GLCCT	QKA
A. fulgidus II	AHTAHARHLVDHLIE	GHNV	GICCT	HKA
R. rubrum	AHSEHGRHIALAMQH	GHNP	GICCT	EKA
C. thermoaceticum	AHCEHGNHIAHALVE	GHNP	GICCT	GKA
C. hydrogenoformans	GHSGHAKHLAHTLKK	GHNP	GICCT	EKA
C. difficile I	AHSDHARDIAHTL…A	GHNP	GMCCT	EKA
C. acetobutylicum I	TYSHHAYEAYRTLKA	GHNP	GSIET	QKA
A. fulgidus III	AYTYHAIEAAKTLKA	GHNP	GFIET	QKA
C. acetobutylicum II	CYVHVVETTARNLKA	GHNH	GCTCV	EQA
C. difficile II	CYLHVVENTAKNLKN	GHNH	GCTCV	EQA
M. jannaschii II	CYVHCAENAARALLS	GHEH	GATCN	EQA
M. kandleri	CYVHCLENAARALKS	GHQM	GATCV	EQA

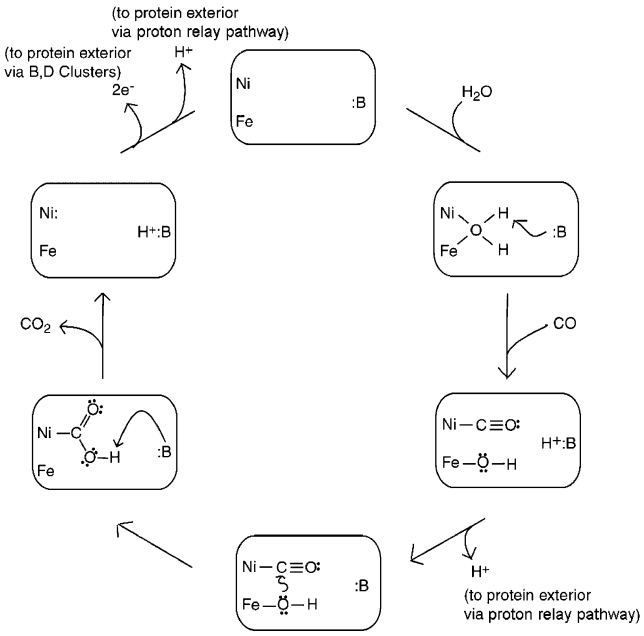

FIGURE 2: Mechanism of CO oxidation, emphasizing proton and electron transfers. Ni and Fe represent the [Ni Fe] subsite of the C-cluster while :B represents a base used in catalysis.

conserved in most (although not all) CODH sequences (*6*) (Table 1).

During the catalytic oxidation of CO to CO_2, water probably binds in bridging fashion to the Ni and unique Fe in a redox state of the C-cluster called C_{red1} (*7*). An unidentified base near the C-cluster abstracts a proton from water, and CO binds to the Ni. The resulting nucleophilic hydroxyl group attacks the carbon of Ni−CO, forming a Ni-bound carboxylate. Either the same or a different base abstracts the proton of this carboxylate, leading to dissociation of CO_2 and the two electron reduction of the cluster, thereby forming a state of the C-cluster called C_{red2}. C_{red1} and C_{red2} states exhibit characteristic EPR signals with $g_{av} = 1.82$ and 1.86, respectively (*8*, *9*). An $[Fe_4S_4]$ D-cluster bridges the two β subunits and is surface-exposed while an $[Fe_4S_4]$ B-cluster is located within each β subunit roughly along a line between the C-clusters and the D-clusters, with clusters spaced ~12 Å apart.

Redox properties of the B- and D-clusters and their position and spacing relative to the active site C-cluster unambiguously identify them as constituting an electron transfer pathway between the C-cluster and the redox partners external to the enzyme. In contrast, little is known about the base(s) used to abstract protons during catalysis or about the pathway used to transfer protons between the C-cluster and the protein surface. Alignment of the 18 CODH primary sequences reported (*6*) reveals the four semiconserved histidine residues His113, His116, His119, and His122. Because of its proximity to the C-cluster, Drennan et al. suggested that His95 of $CODH_{Rr}$ (corresponding to His113 of $CODH_{Mt}$) might act as a catalytic base (*4*). They noted that this residue was positioned at the top of a putative cationic tunnel lined by residues His98, His101, and His108 of $CODH_{Rr}$ (corresponding to His116, His119, and Glu126 of $CODH_{Mt}$). They also suggested that Lys568 of $CODH_{Rr}$ (corresponding to Lys587 of $CODH_{Mt}$) could stabilize a metal-bound carboxylate intermediate during catalysis.

In this study, we tested these hypotheses using site-directed mutagenesis, enzyme activity assays, and EPR spectroscopy. We also examined the effect of mutating the cysteine residue involved in persulfide bond formation. Our results indicate that the persulfide-associated cysteine residue is required for catalysis and possibly for C-cluster assembly or stability. Our evidence also suggests that the four His residues as well as Lys587 and Asn284 are indeed used as a catalytic base and a proton relay network.

EXPERIMENTAL PROCEDURES

Oligonucleotides used to construct mutants were synthesized in the Gene Technologies Laboratory at Texas A&M University. Mutants were constructed using the QuikChange site-directed mutagenesis method from Stratagene, using plasmid pTM02, which contains the genes *acsA* and *acsB*, as the template (*10*). Double mutants were constructed using one oligonucleotide containing both mutations, except for Asn284Ala:His119Ala and Lys587Ala:His113Ala, for which

Table 2: CO Oxidation Activities of $CODH_{Mt}$ Mutant Proteins[a]

	CO oxidation activity (units/mg)					averaged % activity relative to WT
	pH 5.0	pH 6.0	pH 7.0	pH 8.0	pH 9.0	
WT (control for His)	16	43	100	170	300	100
His113Ala	8.0	19	50	70	110	44
His116Ala	2.2	2.8	3.2	5.3	6.6	6
His119Ala	5.0	0.1	35	50	79	27
His122Ala	0.7	0.5	5.2	2.7	6	3
His113Ala + imidazole		19	52	65		45
His116Ala+ imidazole		1.0	3.0	5.0		3
His116Cys	9.5	19	48	69	120	46
His116Asp	0.1	0.2	0.4	0.6	1	0.4
His113Ala:His119Ala	6.0	8.0	9.0	9.0	10	15
H113A:H116A:H119A	0.0	0.0	0.0	0.0	0.0	0.0
Glu115His:His116Ala	3.8	10	22	47	75	24
His116Ala:Gly117His	0.3	0.3	0.6	0.8	1.3	0.8
His122Ala:Ala123His	16	38	62	93	170	72
Ala121His:His122Ala	2.3	4.7	10	18	34	11
Asn284Ala	6.4	26	39	58	94	41
Asn284Ala:His119Ala	4.8	15	42	66	103	36
Lys587Ala:His113Ala	0.1	0.3	0.7	1.3	2.5	0.7
WT (control for C316)				203		100
Cys316Ser				0.6		0.3
WT (control for K568)				170		100
Lys587Ala				73		42

[a] Activities were determined as described in the Experimental Procedures. Three different and independent WT preparations were used as controls for calculating the percentage activities of His, Cys, Asn, and Lys mutants. One unit of activity corresponds to 1 mmol of CO consumed per mg of $CODH_{Mt}$ per min.

two different oligonucleotides were used in two different PCR reactions. All mutant plasmids were produced using an MJ Research Minicycler PCR machine. Mutants were transformed, expressed, harvested, and purified as described (*10*). Protein concentrations were determined by the Biuret method (*11*). Standard CO oxidation activity assays at pH 8 were performed as described (*12*). Other assays were performed identically except at pH 5 (in sodium acetate buffer), pH 6 (in MES), pH 7, and pH 9 (in Tris-HCl). Mutants His113Ala and His116Ala were incubated with 50 mM imidazole (final concentration) for 1 h and then assayed for activity in standard assay buffer. EPR and electronic absorption spectra were obtained as described (*10*). Metal analyses were performed by digesting WT and mutant $CODH_{Mt}$ samples overnight in trace metal grade nitric acid (Fisher), and then analyzing them on a Perkin-Elmer Elan DRC II ICP-MS.

RESULTS

Proton Transfer Mutants. The mutant $CODH_{Mt}$ proteins listed in Table 2 were constructed and isolated as described in the Experimental Procedures. In each case, purity was >80% and the recombinant proteins were soluble in standard buffers. Proteins were brown, indicating the presence of Fe−S clusters. Mutant proteins His113Ala:His122Ala, His116Ala, Glu115His:His116Ala, His119Ala, His122Ala: Ala123His, Lys587Ala, and Asn284Ala exhibited the well-characterized EPR signals from B/D- and C-clusters (Figure 3). The high yields, solubility, color, and EPR spectra indicate that these mutant proteins were properly folded and had the standard set of metal centers found in WT enzyme.

CO oxidation activities for each mutant were obtained in solutions buffered at various pH values (Table 2), except for Lys587Ala and Cys316Ser (see below) whose activities were determined only at pH 8. Activities generally increased as pH increased, consistent with the thermodynamic influence

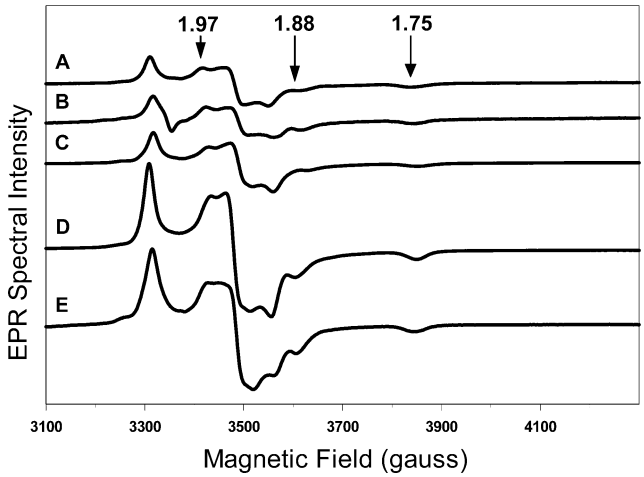

FIGURE 3: EPR spectra of mutants used to identify a proton pathway in $CODH_{Mt}$. (A) His113Ala:His122Ala, (B) His116Ala, (C) His119Ala, (D) Asn284Ala, and (E) Lys587Ala. Arrows from left to right indicate the $g_{av} = 1.86$ signal from the C_{red2} state of the C-cluster. X-band EPR at 10 K was essentially performed as described (*10*).

of generating protons as a product of reaction 1. Deleting each of the four semiconserved His residues had different effects on activity. Activity was nearly abolished in the two mutant proteins where Ala replaced His116 and His122. In contrast, activity was attenuated relative to WT but still significant in mutants where Ala replaced His113 and His119. This latter behavior suggests that these residues are involved in catalysis but may serve redundant functions with other groups. The relative activity of the double mutant with both of these residues replaced with Ala (i.e., His113Ala: His119Ala) was close to the product of the relative activities of the individual mutants (44% × 27% ≈ 15% as observed). Activities of Lys587Ala and Asn284Ala mutants were significant but attenuated relative to WT.

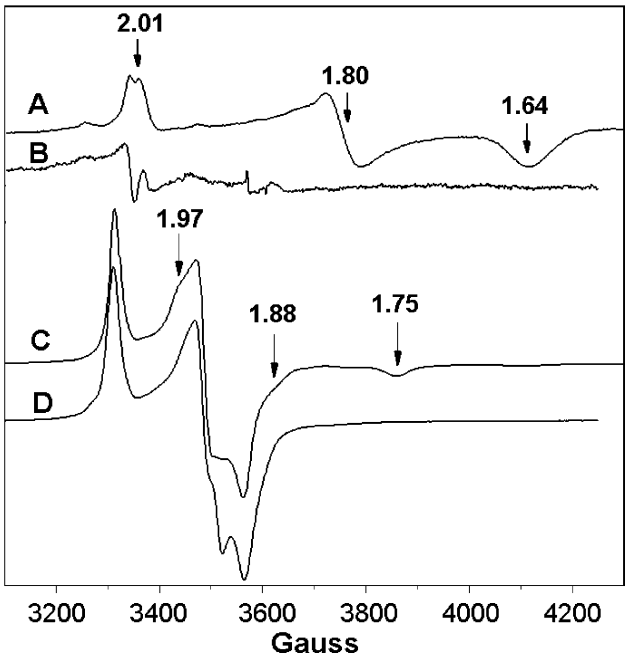

FIGURE 4: EPR showing effect of Cys316 on C-cluster EPR signals. (A) WT recombinant $CODH_{Mt}$ (188 μM) oxidized with a slight molar excess of thionin. Individual g values for the $g_{av} = 1.82$ signal (0.19 spin/$\alpha\beta$) from C_{red1} are given by the arrows. (B) Cys316Ser (316 μM) oxidized with a slight molar excess of thionin. (C) The same as in panel A except reduced by dithionite. Individual g values for the $g_{av} = 1.86$ signal (0.15 spin/$\alpha\beta$) from C_{red2} are given by the arrows. (D) The same as in panel B except reduced by dithionite. EPR conditions were the same as in Figure 3.

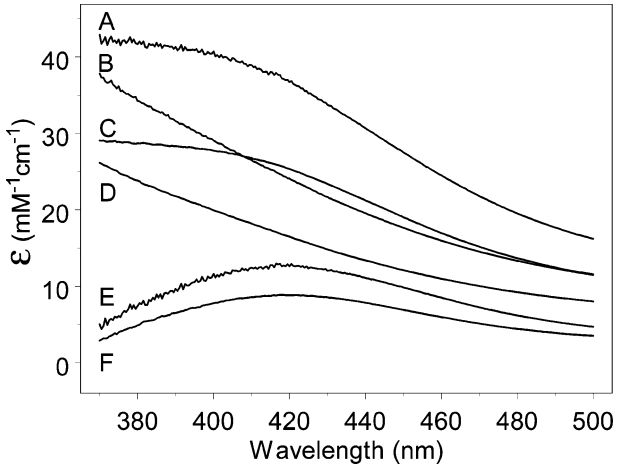

FIGURE 5: Electronic absorption spectra of WT recombinant $CODH_{Mt}$ and Cys316Ser. (A) WT $CODH_{Mt}$ (44 μM $\alpha\beta$) oxidized with a slight excess of thionin. (B) The same as in panel A but reduced with 20 molar equivalents of dithionite. (C) Cys316Ser (32 μM $\alpha\beta$) oxidized with a slight excess of thionin. (D) The same as in panel C but reduced with 20 molar equivalents of dithionite. (E) Difference spectrum of A − B. (F) Difference spectrum of C − D.

Table 3: Characterization of Cys316Ser Mutant $CODH_{Mt}$

	metal analysis (/$\alpha\beta$)		spin quantification of $g_{av} = 1.94$ EPR signal	$\Delta\epsilon_{420}$
	Ni	Fe	(spins/$\alpha\beta$)	($mM^{-1}\,cm^{-1}$)
$CODH_{Mt}$	1.2	13	0.6	12.6
Cys316Ser	0.1	9	0.6	8.9

Activity was not "rescued" by incubating His116Ala or His113Ala in buffer containing imidizole. However, double mutants Glu115His:His116Ala, His122Ala:Ala123His, and Ala121His:His122Ala did exhibit significant activity (Table 2). These endogenous rescue experiments suggest that the function(s) of His116 and His122 do(es) not depend on their exact location. The substantial recovery of activity with double mutant His122Ala:Ala123His is congruent with the fact that some CODHs have a conserved His residue at position 123 instead of 122 (Table 1). Mutant His116Cys also exhibited substantial activity, indicating that Cys can partially mimic the function of His. Like His, Cys has an ionizable hydrogen in its R group and can serve as a general base.

Characterization of Cys316Ser. Three batches of mutant Cys316Ser exhibited an average specific activity <1 unit/mg. A batch of WT recombinant $CODH_{Mt}$, prepared under essentially identical conditions, exhibited a specific activity of 200 units/mg and had standard EPR signals from the B/D- and C-clusters (Figure 4). Cys316Ser exhibited the $g_{av} = 1.94$ signal from the B_{red} state, with an intensity comparable to that from WT $CODH_{Mt}$, but no EPR signals from the C-cluster. Electronic absorption spectra of this mutant suggested that there are 30% fewer Fe−S clusters in the mutant, assuming the same extinction coefficients for each cluster (Figure 5 and Table 3). The mutant lacked significant amounts of Ni and ~30% less Fe relative to WT recombinant protein (Table 3). Note that the A-cluster is largely devoid of Ni in these recombinant proteins (*10*) and so the observed Ni should reflect that present in the C-cluster.

DISCUSSION

Our results suggest that His113, His116, His119, His122, Asn284, and possibly Lys587 are bases involved in proton transfer processes, supporting the initial proposal of Drennan et al. (*4*). The evidence is as follows. First, these residues contain groups that could serve as general bases, and they are conserved in most CODHs and are located roughly in a line between the C-cluster and the protein exterior. Their conserved nature extends beyond primary sequence, as illustrated in the structural comparisons shown in Figure 6. All of this is as would be expected, if these residues functioned as the bases used to abstract protons from the C-cluster (during CO oxidation) and to transfer those protons to solvent. Second, we found that replacing any of these residues with Ala diminished or abolished CO oxidation activities, and that the effect was not due to protein misfolding or to the absence of metal centers in the proteins. Third, the activity could be rescued by replacing some of these residues with others that also have the capacity to serve as bases or by placing His residues in adjacent positions. We will assume such roles for the remainder of this discussion.

We initially assumed that protons would be transferred through a linear pathway where each residue of the pathway would be absolutely required (i.e., where replacing any member of the pathway with a residue that could not serve as a base would abolish activity). Although replacing His116 and His122 with Ala did essentially abolish activity, replacing others (His113 and His119) with Ala lowered activity but did not abolish it. The observed behavior suggests that protons are transferred through a network where some

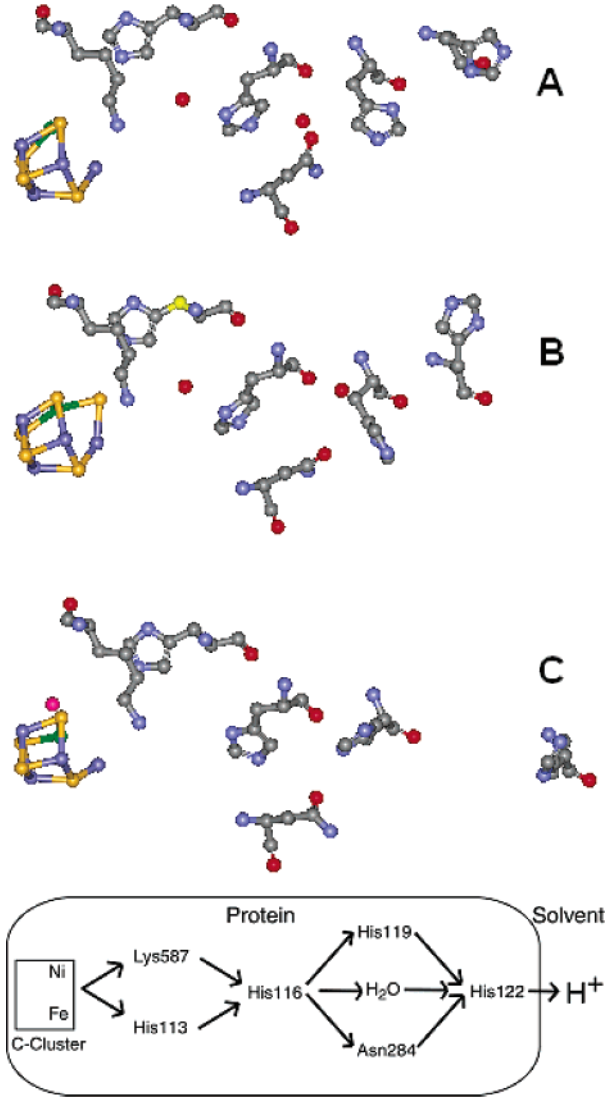

FIGURE 6: Proposed proton network in CODH. Top: Alignment of proton network residues in (A) $CODH_{Mt}$ (*5*), (B) $CODH_{Ch}$ (*2*), and (C) $CODH_{Rr}$ (*4*) including two ordered waters. Corresponding alignment for $CODH_{Mt}$ (*3*) is indistinguishable from $CODH_{Mt}$ (*5*). Bottom: Proposed network, using residue numbering for $CODH_{Mt}$.

members of that network serve redundant roles and others serve nonredundant (or required) roles. Redundant bases would accept protons from a common donor and donate them to a common acceptor. The requirement for His116 and His122 suggests that they play nonredundant roles while the partial requirement for His113 and His119 suggests that they play redundant roles. These considerations constitute the foundation of our proton network model (Figure 6, bottom).

His113 is located nearest to the C-cluster, suggesting that it serves as the base used to abstract a proton from (i) water bound to the unique Fe during one step of catalysis and from (ii) a Ni-bound carboxylate in another step of catalysis. However, the partially required nature of this residue suggests that another group might serve the same role. Lys587 is located near to the [Ni Fe] subsite of the C-cluster and has been proposed to stabilize the Ni-bound carboxylate intermediate (*4*). The partial loss of activity in the mutant with this residue replaced with Ala is consistent with this proposal if the caveat that another group exists that plays a redundant role is included. The near complete abolition of activity when Lys587 and His113 were replaced with Ala is more dramatic than would be expected if both residues served separate functions with other redundant groups. In this case, the activity of the double mutants would be the product of the activities of the individual mutants—namely, 44% × 42% = 21% of relative activity. The observed activity (0.7%, relative to WT) suggests that His113 and Lys587 serve the same function—that is, they are an exclusive redundant pair. This suggestion is included in the model of Figure 6. Another possible redundant base to consider is water, in that there are two conserved water molecules within this region of the WT protein (*2*, *3*, *5*) and additional waters might be present in mutant proteins.

His116 is required for catalysis, and its location suggests that it accepts a proton from His113 (and from any redundant donor such as Lys587). According to our model, His116 donates a proton to either of three redundant acceptors, including His119, Asn284, and an unidentified acceptor, viewed in the model as one of the ordered waters present in the WT structure. We include a third redundant pathway to explain the substantial activity of the double mutant Asn284Ala:His119Ala. These three redundant groups then donate protons to His122, a required residue that appears to be nonredundant, and then, His122 donates protons to the solvent or an unidentified exogenous base.

Despite ambiguity as to some of the specific residues involved in this pathway, the location of those residues considered here indicates that the proton transfer pathway is distinct from the electron transfer pathway involving the B- and D-clusters. This distinction is illustrated in Figure 7. Similarly distinct proton and electron pathways are evident in the Ni hydrogenase from *Desulfovibrio gigas* (*13*) and in the iron-only hydrogenase from *Clostridium pasteurianum* (*14*). The former enzyme contains four His (three of which are highly conserved) residues and a conserved Glu connecting the active site [Ni Fe] center to the surface; they apparently constitute a proton relay pathway. The location of this pathway differs significantly from the two Fe_4S_4 clusters and one Fe_3S_4 cluster used to transfer electrons between the active site and the surface. In the iron-only hydrogenase, electrons are transferred from the [Fe Fe] active site to the surface via Fe_4S_4 and Fe_2S_2 clusters, while protons are transferred via a free Cys residue, two Glu's, and a Ser (*14*). These similarities raise the possibility that separate proton and electron transfer pathways will be found whenever a series of Fe−S clusters constitute the electron transfer pathway.

Our results also demonstrate that Cys316 is required for catalytic activity, although the origin of its effect remains elusive. Prior to a referee's comment (and to performing metal and UV−vis analyses), we had concluded that the persulfide bond formed between Cys316 and a sulfide of the $[Fe_3S_4]$ subsite of the C-cluster allowed development of the C_{red1} and C_{red2} redox states. This explanation was consistent with the EPR spectra of this mutant and with previous studies, which indicated heterogeneous populations of C-clusters. For example, the spin intensity of the C_{red1} and C_{red2} EPR signals of WT enzyme quantifies to only 0.2−0.3 spins/$\alpha\beta$ rather then the expected value of unity (*8*). Redox titrations indicated that only those C-clusters that exhibit the C_{red1} and C_{red2} states can be reduced by three electrons, namely, from C_{ox} to C_{red1} and then from C_{red1} to

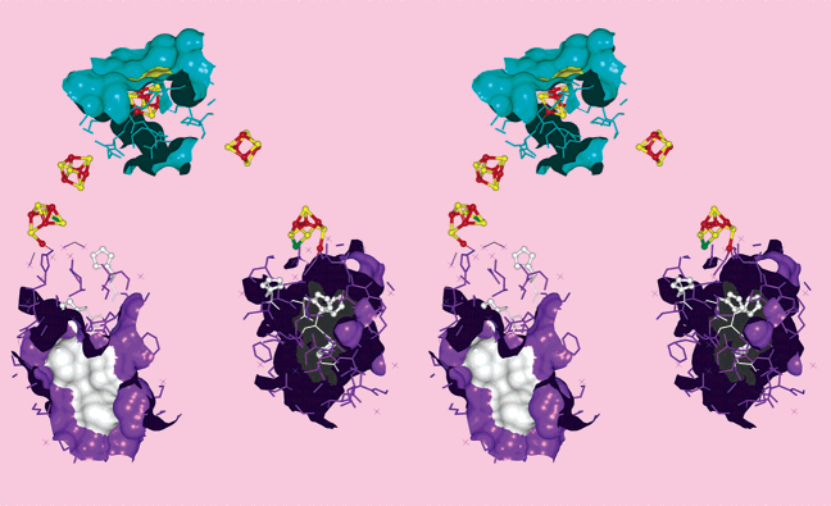

FIGURE 7: Stereoview showing distinct proton and electron transfer pathways through $CODH_{Mt}$. The cluster with the green ball (Ni) is the C-cluster. During CO oxidation catalysis, electrons are transferred from the C-cluster to the B-cluster (located above and to the left of the C-cluster) and then to the D-cluster (located on the protein surface, given in turquoise) and out of the protein. In contrast, protons are transferred from the C-cluster to the relay network including His residues (shown in white).

C_{red2} states; the remainder are reducible by just one electron, namely, from C_{ox} to an $S = 3/2$ state (*9*). We initially suspected that the low spin intensities and heterogeneous redox activity arose because only 20−30% of C-clusters had a persulfide bond.

However, after we performed metal and UV−vis analyses, our results now suggest that replacing Cys316 with Ser results in a mutant protein lacking the C-cluster entirely! If true, Cys316 would appear to function either in the assembly or stability of the C-cluster. It also suggests that $CODH_{Mt}$ is stable in the absence of the C-cluster. One possibility is that the persulfide bond is used in the assembly of the C-cluster and that the reduction of this bond is one of the last steps in this assembly process. Viewed from this perspective, the fraction of molecules containing this bond as found crystallographically in a fraction of C-clusters would be a remnant of an incomplete assembly process. Further studies are clearly required to evaluate this possibility.

Finally, we note that CODH sequences that contain the conserved His, Lys, and Asn residues, which are involved in the proton pathway, also contain the cysteine residue involved in persulfide bond formation. Moreover, CODH sequences lacking the proton pathway residues also lack the Cys involved in persulfide bond formation; a horizontal line separates these two groups in Table 1. This implies that the proton pathway and the C-cluster structure itself are either present or absent for a given protein. Given that the mutant $CODH_{Mt}$ lacking the C-cluster appears to be stable, we propose that proteins lacking these residues (i.e., the sequences below the line in Table 1) are not enzymes that catalyze reaction 1—that is, they are not CODHs. Although further studies are required to examine this proposal, it is consistent with a report that cell extracts of one of the organisms, which contain two of these below-the-line sequences (*Clostridium acetobutylicum*), do not exhibit CO oxidation activity (*15*).

ACKNOWLEDGMENT

Lisa M. Pérez at the Laboratory for Molecular Simulation (LMS) kindly generated the stereoimage using Insight II 2000 (Accelrys, Inc.). We also acknowledge the LMS for providing the software and hardware necessary to prepare the stereoimage.

REFERENCES

1. Lindahl, P. A. (2002) The Ni-Containing Carbon Monoxide Dehydrogenase Family: Light at the End of the Tunnel?, *Biochemistry 41*, 2097−2105.
2. Dobbek, H., Svetlitchnyi, V., Gremer, L., Hubber, R., and Meyer, O. (2001) Crystal Structure of a Carbon Monoxide Dehydrogenase Reveals a [Ni-4Fe-5S] Cluster, *Science 293*, 1281−1285.
3. Doukov, T. I., Iverson, T. M., Seravalli, J., Ragsdale, S. W., and Drennan, C. L. (2002) A Ni-Fe-Cu Center in a Bifunctional Carbon Monoxide Dehydrogenase/Acetyl-CoA Synthase, *Science 298*, 567−572.
4. Drennan, C. L., Heo, J., Sintchak, M. D., Schreiter, E., and Ludden, P. W. (2001) Life on Carbon Monoxide: X-ray Structure of *Rhodospirillum rubrum* Ni-Fe-S Carbon Monoxide Dehydrogenase, *Proc. Natl. Acad. Sci. U.S.A. 98*, 11973−11978.
5. Darnault, C., Volbeda, A., Kim, E. J., Legrand, P., Vernede, X., Lindahl, P. A., and Fontecilla-Camps, J. C. (2003) Ni-Zn-[Fe4S4] and Ni-Ni-[Fe4S4] Clusters in Closed and Open Subunits of Acetyl-CoA Synthase/Carbon Monoxide Dehydrogenase, *Nat. Struct. Biol. 10*, 271−279.
6. Lindahl, P. A., and Chang, B. (2001) The Evolution of Acetyl-CoA Synthase, *Origins Life Evol. Biosphere 31*, 403−434.
7. Feng, J., and Lindahl, P. A. (2004) Carbon Monoxide Dehydrogenase from *Rhodospirillum rubrum*: Effect of Redox Potential on Catalysis, *Biochemistry 43*, 1552−1559.
8. Lindahl, P. A., Münck, E., and Ragsdale, S. W. (1990) CO Dehydrogenase from *Clostridium thermoaceticum*; EPR and Electrochemical Studies in CO_2 and Argon Atmospheres, *J. Biol. Chem. 265*, 3873−3879.
9. Fraser, D. M., and Lindahl, P. A. (1999) Stoichiometric CO Reductive Titrations of Acetyl-CoA Synthase (Carbon Monoxide Dehydrogenase) from *Clostridium thermoaceticum*, *Biochemistry 38*, 15697−15705.
10. Loke, H. K., Bennett, G., and Lindahl, P. A. (2000) Active Acetyl-CoA Synthase from *Clostridium thermoaceticum* Obtained by Cloning and Heterologous Expression of *acsAB* in *Escherichia coli*, *Proc. Natl. Acad. Sci. U.S.A. 97*, 12530−12535.
11. Pelley, J. W., Garner, C. W., and Little, G. H. (1978) Simple Rapid Biuret Method for Estimation of Protein in Samples Containing Thiols, *Anal. Biochem. 86*, 341−343.
12. Shin, W., and Lindahl, P. A. (1993) Low Spin Quantitation of NiFeC EPR Signal from Carbon Monoxide Dehydrogenase Is Not Due to Damage Incurred During Protein Purification, *Biochim. Biophys. Acta 1161*, 317−322.

13. Volbeda, A., Charon, M. H., Piras, C., Hatchikian, E. C., Frey, M., and Fontecilla-Camps, J. C. (1995) Crystal Structure of the Nickel−Iron Hydrogenase from *Desulfovibrio gigas*, *Nature 373*, 580−587.
14. Peters, J. W., Lanzilotta, W. N., Lemon, B. J., and Seefeldt, L. C. (1998) X-ray Crystal Structure of the Fe-Only Hydrogenase (Cpl) from *Clostridium pasteurianum* to 1.8 Angstrom Resolution, *Science 282*, 1853−1858.
15. Kim, B. H., Bellows, P., Datta, R., and Zeikus, J. G. (1984) Control of Carbon and Electron Flow in *Clostridium acetobutylicum* Fermentations−Utilization of Carbon Monoxide To Inhibit Hydrogen Production and To Enhance Butanol Yields, *Appl. Environ. Microbiol. 48*, 764−770.

BI036062U